

## Atomic structure of the reactive Fe/Si(111)7×7 interface

A. Mascaraque

*Departamento de Física de la Materia Condensada and Instituto Universitario de Ciencia de Materiales "Nicolás Cabrera,"  
Universidad Autónoma de Madrid, 28049 Madrid, Spain*

J. Avila, C. Teodorescu, and M. C. Asensio

*LURE, Bâtiment 209D, Université Paris-Sud, F-91405 Orsay, France  
and Instituto de Ciencia de Materiales, CSIC, 28049 Madrid, Spain*

E. G. Michel

*Departamento de Física de la Materia Condensada and Instituto Universitario de Ciencia de Materiales "Nicolás Cabrera,"  
Universidad Autónoma de Madrid, 28049 Madrid, Spain*

(Received 24 October 1996)

The early stages of Fe/Si(111) interface formation have been investigated using x-ray photoelectron diffraction. Deposition of Fe in the range of one monolayer on Si(111)7×7 at room temperature results in the destruction of the 7×7 reconstruction. After a slight anneal, a well ordered interface is formed. This reacted layer is terminated by a top Si bilayer, which is rotated 180° with respect to the substrate stacking sequence. Fe atoms occupy substitutional Si lattice sites in the next bilayer underneath, keeping an interface coordination similar to the eightfold type. Thus, this initial interface already exhibits several of the most important features of thicker epitaxial silicide films. This result is evidence of the importance of the earliest stages of epitaxial growth to understand the properties of thicker layers. [S0163-1829(97)53112-2]

The growing interest in the application of silicides to microelectronics has widened the scope of silicide research and opened up many avenues of investigation.<sup>1,2</sup> In this respect, iron silicides have deserved special attention due to their interesting properties. Thus,  $\beta$ -FeSi<sub>2</sub> is one of the few semi-conducting silicides,<sup>3</sup> and  $\epsilon$ -FeSi has been proposed as the first example of a *d*-electron based Kondo insulator.<sup>4</sup> Furthermore, metastable iron silicides can be epitaxially grown on Si(111).<sup>5,6</sup> These are compounds not found in the bulk phase diagram, stabilized by the epitaxy due to their better lattice matching with the substrate. The most interesting example is FeSi(CsCl). Its structure admits a range of Fe:Si stoichiometries by introducing Fe or Si vacancies in the lattice.<sup>7</sup> The Fe-richest phases may present magnetic ordering. But even non-magnetic FeSi<sub>1+x</sub> has novel properties: Fe/FeSi<sub>1+x</sub>/Fe superlattices are antiferromagnetically coupled for a range of spacer thickness.<sup>8,9</sup> These properties are strongly related to the crystalline nature of the silicide layer and the silicide/Si interface, which critically determine the coupling transmission through the spacer.

In this paper we describe the structure of the reactive Fe/Si(111)7×7 interface at its earliest stages using the information provided by x-ray photoelectron diffraction (XPD). The first step of room temperature (RT) reaction is the penetration of Fe in the Si lattice to occupy substitutional sites. A moderate anneal results in the formation of a well ordered intermixed layer, terminated by a silicon bilayer. Fe atoms selectively occupy subsurface Si sites in the first bilayer underneath the top Si bilayer. Our results show that the Si bilayer is 180° rotated (type-B orientation<sup>10</sup>), and demonstrate this preferential orientation from the earliest stages of growth. This is also true for the interface metal atoms coordination number. The structure found reflects the first stages of formation of an interface based on eightfold coordinated Fe atoms.<sup>2</sup> This result is a clear-cut example of the importance of first metal-atoms reaction to determine interface properties.

The outgoing wave field in a photoemission experiment is diffracted by atoms in the vicinity of the emitter. This phenomenon is used in the XPD technique. We refer the reader to Ref. 11 for more details. The experimental intensity modulations were compared in this work with the results of a suitable scattering formalism that simulates the measured XPD by modeling the structure of the interface.<sup>12</sup> A spherical-wave single-scattering cluster (SSC) formalism was adequate to reproduce the data<sup>13</sup> and discern the correct structural model, obtained from a systematic search. We used a cluster of 2000 atoms, with a mean-free-path dependent attenuation of the electron yield, calculated according to Ref. 14. Simulated XPD patterns were generated with emitters at symmetry-inequivalent sites in the first to fifth top-most interface layers. The Si and Fe muffin-tin scattering phase shifts were used and the inner potential was 10 eV. Spherical-wave multiple-scattering cluster (MSC) calculations were also performed, and the best model found from SSC calculations was refined within a MSC scheme (see below).

The experiments were performed in one ultrahigh vacuum chamber (base pressure:  $5 \times 10^{-11}$  mbar) equipped with an angle resolving hemispherical analyzer and a high precision manipulator that permits rotation in the full 360° azimuthal emission angle ( $\Phi$ ) and 180° polar emission angle relative to the surface ( $\Theta$ ). The azimuthal XPD scans were made by rotating the sample around its normal and recording the Si 2*p* and Fe 3*p* intensities every 2° at fixed  $\Theta$ , with an absolute angular precision of 0.5° for both  $\Theta$  and  $\Phi$ . The photoelectron intensity was recorded at a constant kinetic energy, defined as an integrated peak area above a linear background. The anisotropy of the XPD curves has been defined as  $\chi = (I_{max} - I_{min})/I_{min}$ . The XPD patterns were recorded using 400 eV photons from the SU7-TGM beamline of Super-Aco storage ring in Orsay. In all experiments, the Si(111)

*p*-doped sample was heated up for degassing to 650 °C for several hours by resistive heating and then flashed at 1100 °C for 15 s in order to get a clean Si(111)7×7 surface. Fe coverage (accuracy ±15%) was measured with a quartz crystal and cross checked by a quantitative comparison of Fe and Si core levels.<sup>15</sup> We define in this paper 1 ML coverage as an amount of atoms equal to the Si(111) surface density ( $7.85 \times 10^{14}$  atoms/cm<sup>2</sup>).

Although not much is known about the earliest stages of deposition of Fe on Si(111) at RT, the data presented here agree well with existing information on this and related systems. It seems established that the interface is reactive and an initial silicide layer of unknown structure is formed.<sup>16</sup> Low-energy ion scattering and scanning tunneling microscopy experiments revealed that for Fe coverages below 2 ML, the surface is Si terminated.<sup>16</sup> In the case of thicker epitaxial films, a type-*B* orientation has been found for FeSi(CsCl) layers.<sup>17–19</sup> An initial reacted layer was found also in the case of RT deposition of Ni or Co on Si(111).<sup>10,20,21</sup>

Figure 1 shows the evolution of Si 2*p* and Fe 3*p* 360°-azimuthal scans for  $\Theta=40^\circ$  obtained upon annealing 1 ML Fe deposited at RT. An inspection of these curves reveals the following features: (1) The intense Si 2*p* XPD peaks along the  $\langle 211 \rangle$  directions, derived from the stacking fault in the 7×7 unit cell,<sup>22</sup> are strongly attenuated after Fe deposition, even at RT [Fig. 1(a)]. (2) The Fe XPD pattern presents a rich anisotropy already at RT, indicative of an ordered Fe reacted layer. (3) The ordering is improved by a slight annealing to 150 °C. In these conditions the modulation of the Fe signal shows two set of three-fold symmetry peaks, while the Si XPD pattern presents only three strong peaks along the  $\langle 121 \rangle$  directions, characteristic of a Si(111)1×1 structure (see below). (4) A further anneal up to 250 °C diminishes the ordering of the reacted interface. The modulations disappear completely after annealing to temperatures above 450 °C due to diffusion of Fe in the Si crystal.<sup>15</sup> In view of this behavior, we concentrate on the following on the interfaces annealed to 150 °C.

In order to determine the atomic structure of the ordered interface, a whole 360°  $\Phi$ -angle range was probed for more than 25 different  $\Theta$  angles at steps of 2°, recording both Si 2*p* and Fe 3*p* core levels. These experimental scans were compared to the simulations obtained from different models for the interface. The agreement between experimental and simulated traces was evaluated calculating the reliability factor  $R_m$  (Ref. 23) defined in Ref. 24.  $R_m$  measures how well the experimental curve is reproduced by the simulation. A lower  $R_m$  corresponds to a better agreement. Figure 2 presents a set of selected simulated azimuthal and experimental XPD patterns at  $\Theta=40^\circ$ , both for Fe 3*p* and Si 2*p*. In order to develop the interface models we keep in mind that the Fe 3*p* azimuthal scans systematically reproduce the same Si 2*p* XPD modulations along the  $\langle 121 \rangle$  directions (see also Fig. 1). This behavior suggests that Fe and Si atoms occupy sites of similar local environment, either by Fe substitutional occupation of Si lattice sites, or by formation of a silicide, where Fe and Si sites are of identical nature.<sup>25</sup> We have first tested models based on the formation of an intermixed layer with substitutional occupation of Si sites by Fe atoms, terminated by a Si bilayer. These structures cannot account for the experiment, as evidenced by the poor agreement of traces (a)

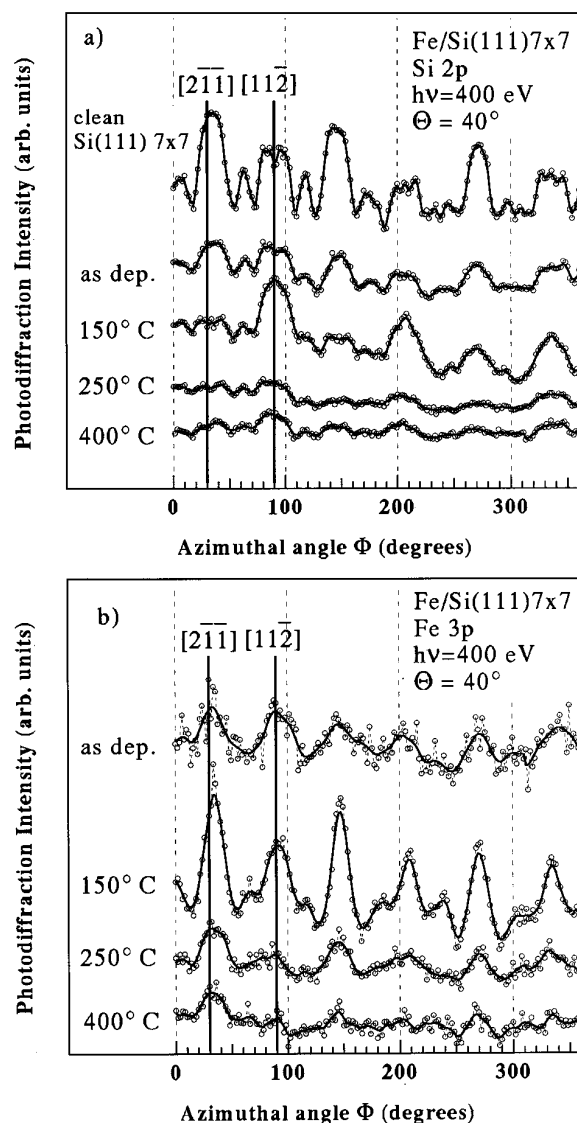


FIG. 1. Experimental azimuthal scans for Si 2*p* [panel (a)] and Fe 3*p* [panel (b)] vs annealing temperature for 1 ML Fe deposited on Si(111). Continuous lines are a guide to the viewer. The large intensity modulations found at 150 °C evidence a well-ordered interface.  $\Phi=0^\circ$  corresponds to the [110] direction.

( $R_m=0.299$ ), (b) ( $R_m=0.233$ ), and (c) ( $R_m=0.243$ ) in Fig. 2, which correspond to substitutional occupation of third, fourth, and full third+fourth layers by Fe, respectively. In fact, Fe 3*p* XPD patterns display also distinctive strong peaks along the  $\langle 211 \rangle$  directions, which cannot be reproduced in these simple models (see also Fig. 1). Traces (d) ( $R_m=0.259$ ), (e) ( $R_m=0.262$ ), and (f) ( $R_m=0.222$ ) in Fig. 2 correspond to the same conditions as for (a), (b), and (c), respectively, but now the top Si bilayer has been rotated 180° with respect to the Si substrate. The agreement between experiment and model is improved, in particular for the Fe 3*p* traces. The model has been further refined by allowing Fe atoms to occupy partially third and fourth layers. We allowed also the vertical height of the bilayer to relax.<sup>22</sup> This structural optimization was performed within a MSC formalism with the aid of an automatic procedure.<sup>26,27</sup> Multiple parameter scans of the structural parameter space (bilayer relaxation and Fe content) were also investigated using the criteria of a reliability factor minimization.<sup>28</sup> The best agree-

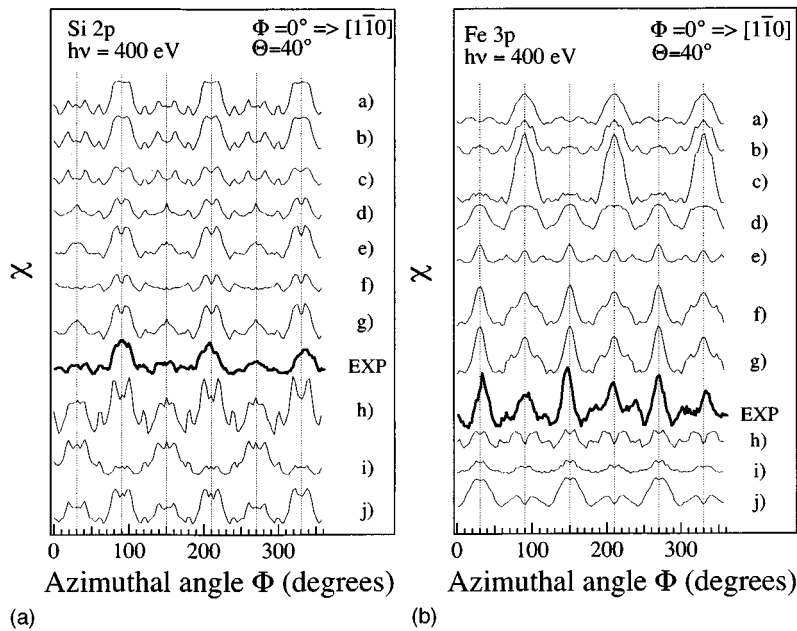


FIG. 2. Comparison between experimental azimuthal scans [1 ML Fe/Si(111) annealed to 150 °C] for (a) Si and (b) Fe (thick traces, denoted EXP), and theoretical simulations using a SSC formalism for different interface structures (thin traces, see text for details). Model (g) presents the best agreement found.  $\chi$  is the photoelectron diffraction asymmetry parameter defined in the text.

ment was found for 50% random occupation of the third and fourth layers by Fe atoms [trace (g) in Fig. 2,  $R_m=0.095$ ] and a bilayer height of 3.01 Å, i.e. close to the bulk value (3.135 Å). The agreement between experimental and simulated traces is now excellent in the whole range of  $\Theta$  angles probed, as shown in Fig. 3,<sup>29</sup> where the result of MSC calculations is shown together with the experiments. The difference with equivalent SSC results was not significant for our experimental conditions.<sup>22</sup>

In spite of the good agreement already found, we have tested as a second possibility whether the experiments could be explained by the formation of one of the known iron silicides. Compounds of this type have been found for higher Fe coverages and annealing temperatures.<sup>5,6</sup> Traces (i) ( $R_m=0.566$ ) and (j) ( $R_m=0.322$ ) in Fig. 2 correspond to Si-terminated  $\gamma$ -FeSi<sub>2</sub>,<sup>6</sup> and FeSi(CsCl),<sup>5</sup> respectively. These models were refined trying to improve the agreement following the guidelines exposed in the previous paragraph, without success. It is clear from traces (i) and (j) of Fig. 2 that

simulated and experimental XPD patterns of Si and Fe are entirely anticorrelated for a silicide, in disagreement with the experiment. This conclusion agrees with photoemission results,<sup>16</sup> which suggest the formation of a phase different from FeSi(CsCl).

The structure found for the reacted layer is illustrated schematically in Fig. 4. This structure explains well all experimental evidence concerning the low-coverage, low-annealing temperature Fe/Si(111) interface. Fe atoms deposited at RT diffuse inwards towards the Si surface, showing already at RT a preferential occupation of Si lattice sites. The fact that only  $\langle 2\bar{1}\bar{1} \rangle$  Si 2*p* peaks are selectively influenced (see Fig. 1) indicates that Fe atoms rapidly degrade the 7×7 reconstruction. Reaction mechanisms based in Si-metal interchanging were proposed long time ago to understand the disruption of the Si covalent bonds after reaction.<sup>30–32</sup> Nevertheless, the Fe/Si intermixed layer is well ordered for adequate preparation conditions at variance with other cases.<sup>20</sup> It is after annealing to 150 °C that the 7×7 reconstruction is

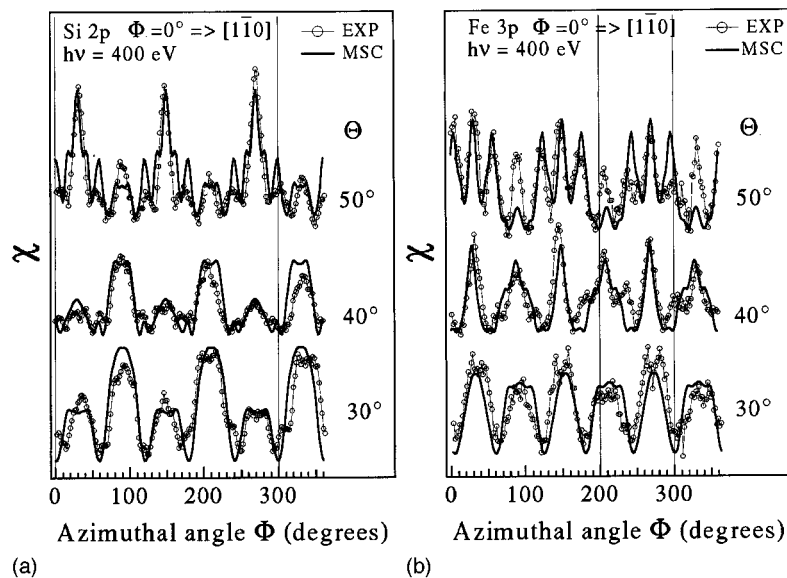


FIG. 3. Comparison between simulated azimuthal scans using a MSC formalism (thick lines) for (a) Si 2*p* and (b) Fe 3*p* [1 ML Fe/Si(111) annealed to 150 °C] and experimental scans (circles), detected for different  $\Theta$  angles. The simulated scans correspond to model (g) from Fig. 2.

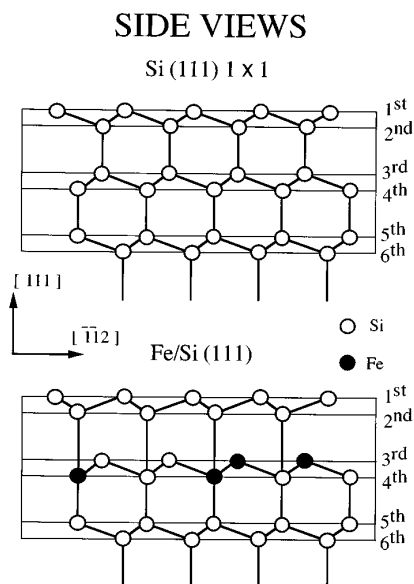


FIG. 4. Top: Si(111)1×1 side view. Bottom: schematic representation of model (g) from Fig. 2. Fe atoms occupy randomly third and fourth layer sites. The top Si bilayer is 180° rotated and keeps the registry shown in the figure with the layer underneath.

substituted by a well-ordered layer terminated by a 180° rotated 1×1 Si bilayer. A Si termination reflects in fact a general trend towards Si outdiffusion observed in transition metal silicides, due to the lower Si surface energy, whenever kinetic limitations do not prevent it.<sup>2</sup> Figure 2 depicts, as well, the strong improvement in the quality of the fit when the top Si bilayer is rotated 180° with respect to the substrate [compare traces (c) and (g) with the experiment]. This rotation can be interpreted as the earliest stage of formation of a type-*B* interface. Our findings indicate that the 180° rotation

involved in a type-*B* orientation takes place already at the monolayer range. Thus, the energy gained in the process would be preserved for thicker films. The registry found<sup>29</sup> leaves third layer Si/Fe atoms with unsaturated bonds (see Fig. 4). Thus, fourth layer atoms have a fivefold coordination, but the interface registry reminds of the eightfold interface coordination found for CoSi<sub>2</sub> grown on Si(111).<sup>33</sup> These results show evidence that attempts to control the silicide orientation or interface structure should concentrate in the earliest stages of deposition and should take into account the particular surface reconstruction of the substrate.

A proper silicide layer [e.g., FeSi(CsCl)] has not been found. The formation of a compound is favored under solid phase epitaxy conditions when the energy gain compensates the substrate bond breaking. Obviously this simple energetic balance may be unfavorable in the low coverage regime. Then, the thickness of the film is too low to allow for an energy gain due to compound formation with a well-matching interface, and an intermixed layer keeping the substrate structure may result in a lower energy.

In summary, we have demonstrated that a well-ordered Fe/Si(111) interface is formed in the ML range. This interface already reproduces several important features of thicker epitaxial films, as a type-*B* orientation, and as an interface coordination, which reminds us of the geometry found in thicker films.

This work was financed by DGICYT (Spain) under Grant No. PB-94-1527 and Grant No. PB-94-0022-C02-01. The access of A.M. and E.G.M. to LURE, Centre Universitaire Paris-Sud, was supported through the Large Scale Facilities program of the European Union. A.M. thanks Eusko Jaurlaritza for financial support. We thank Dr. V. Fritzsche for providing us with the multiple scattering code.

<sup>1</sup>R. Tung, in *Contacts to Semiconductors*, edited by L.J. Brillson (Noyes Publication, New Jersey, 1993).

<sup>2</sup>H. von Känel, *Mater. Sci. Rep.* **8**, 193 (1992), and references therein.

<sup>3</sup>M.C. Bost and J.E. Mahan, *J. Appl. Phys.* **58**, 2696 (1985).

<sup>4</sup>T.E. Mason *et al.*, *Phys. Rev. Lett.* **69**, 490 (1992).

<sup>5</sup>H. von Känel *et al.*, *Phys. Rev. B* **45**, 13 807 (1992).

<sup>6</sup>A.L. Vázquez de Parga *et al.*, *Europhys. Lett.* **18**, 595 (1992).

<sup>7</sup>H. von Känel *et al.*, *Appl. Surf. Sci.* **70/71**, 559 (1993).

<sup>8</sup>E.E. Fullerton *et al.*, *J. Appl. Phys.* **73**, 6335 (1993).

<sup>9</sup>J.E. Mattson *et al.*, *Phys. Rev. Lett.* **71**, 185 (1993).

<sup>10</sup>R.T. Tung, *J. Vac. Sci. Technol. A* **5**, 1840 (1987).

<sup>11</sup>W.F. Egelhof, *CRC Crit. Rev. Solid State Mater. Sci.* **16**, 213 (1990).

<sup>12</sup>J. Osterwalder *et al.*, *Surf. Sci.* **331-333**, 1002 (1995).

<sup>13</sup>C.S. Fadley, in *Synchrotron Radiation Research, Advances in Surface Science*, edited by R.Z. Bachrach (Plenum, New York, 1990).

<sup>14</sup>S. Tanuma, C.J. Powell, and D.R. Penn, *Surf. Interface Anal.* **17**, 927 (1991).

<sup>15</sup>J. Alvarez *et al.*, *Phys. Rev. B* **45**, 14 042 (1992).

<sup>16</sup>J. Alvarez *et al.*, *Phys. Rev. B* **47**, 16 048 (1993).

<sup>17</sup>H. Sirringhaus *et al.*, *Phys. Rev. B* **47**, 10 567 (1993).

<sup>18</sup>U. Kafader *et al.*, *Appl. Surf. Sci.* **64**, 297 (1993).

<sup>19</sup>S. Hong *et al.*, *Appl. Surf. Sci.* **90**, 65 (1995).

<sup>20</sup>C. Pirri *et al.*, *Phys. Rev. B* **29**, 3391 (1984).

<sup>21</sup>L. Luo *et al.*, *Surf. Sci.* **249**, L338 (1991).

<sup>22</sup>A. Mascaraque *et al.* (unpublished).

<sup>23</sup>All  $R_m$  values cited in this paper are obtained adding the six individual  $R_m$ -s calculated in each model for  $\Theta=30^\circ$ ,  $40^\circ$ , and  $50^\circ$  for Fe 3*p* and Si 2*p*.

<sup>24</sup>R. Dippel *et al.*, *Chem. Phys. Lett.* **199**, 625 (1992).

<sup>25</sup>The simulated traces were obtained using bulklike atomic positions, with the exception of the vertical distance of the top Si bilayer, which was allowed to relax in model (g).

<sup>26</sup>V. Fritzsche, *J. Phys., Condens. Matter.* **2**, 9735 (1990).

<sup>27</sup>V. Fritzsche, *J. Electron Spectrosc. Relat. Phenom.* **58**, 299 (1992).

<sup>28</sup>J.B. Pendry, *J. Phys. C* **13**, 937 (1980).

<sup>29</sup>Two different registries are possible for a 180°-rotated top bilayer with respect to the substrate. The first involves bonding between second and fourth layer atoms, as illustrated in Fig. 4 (bottom) and produces trace (g) in Fig. 2 and all the simulated traces shown in Fig. 3. The second possibility involves direct bonding between second and third layer atoms. It corresponds to the simple stacking fault found in a 7×7 reconstruction. This second possibility gives rise to trace (h) ( $R_m=0.243$ ) in Fig. 2. This and related structures were discarded due to their much worse agreement with the experiment.

<sup>30</sup>L.J. Brillson, *Surf. Sci. Rep.* **2**, 123 (1982).

<sup>31</sup>R.J. Hamers and J.E. Demuth, *Phys. Rev. Lett.* **60**, 2527 (1988).

<sup>32</sup>I.W. Lyo, E. Kaxiras, and Ph. Avouris, *Phys. Rev. Lett.* **63**, 1261 (1989).

<sup>33</sup>C.W.T. Bulle-Lieuwma *et al.*, *Appl. Phys. Lett.* **55**, 648 (1989).